Title
Quantifying the Effects of Historical Land Cover Conversion Uncertainty on Global Carbon and Climate Estimates

Journal
Geophysical Research Letters, 45(2)

ISSN
0094-8276

Authors
Di Vittorio, AV
Mao, J
Shi, X
et al.

Publication Date
2018-01-28

DOI
10.1002/2017gl075124

Peer reviewed

Quantifying the effects of historical land cover conversion uncertainty on global carbon and climate estimates

A. V. Di Vittorio[1], J. Mao[2], X. Shi[2], L. Chini[3], G. Hurtt[3], and W. D. Collins[1,4]

[1]Lawrence Berkeley National Laboratory, One Cyclotron Road, MS 74R316C, Berkeley, CA, 94720.

[2]Environmental Sciences Division and Climate Change Science Institute, Oak Ridge National Laboratory, Oak Ridge, TN, USA

[3]Department of Geographical Sciences, University of Maryland, College Park, MD

[4]Department of Earth and Planetary Sciences, University of California, Berkeley, CA

Corresponding author: Alan V. Di Vittorio (avdivittorio@lbl.gov)

Key Points:

- Land cover conversion uncertainty constitutes a 5 ppmv range in estimated atmospheric CO_2 concentrations in 2004
- Land cover conversion uncertainty generates land carbon uncertainty that is 80% of net CO_2 and climate effects on terrestrial carbon stock through 2004
- Land cover conversion uncertainty generates a range in projected local surface temperature of over 1° C (1984-2004 avg)

Abstract

Previous studies have examined land use change as a driver of global change, but the translation of land use change into land cover conversion has been largely unconstrained. Here, we quantify the effects of land cover conversion uncertainty on the global carbon and climate system using the integrated Earth System Model. Our experiments use identical land use change data and vary land cover conversions to quantify associated uncertainty in carbon and climate estimates. Land cover conversion uncertainty is large, constitutes a 5ppmv range in estimated atmospheric CO_2 in 2004, and generates carbon uncertainty that is equivalent to 80% of the net effects of CO_2 and climate and 124% of the effects of nitrogen deposition during 1850-2004. Additionally, land cover uncertainty generates differences in local surface temperature of over 1 °C. We conclude that future studies addressing land use, carbon, and climate need to constrain and reduce land cover conversion uncertainties.

1 Introduction

Global socioeconomic and Earth system modeling efforts, such as phase 5 of the Coupled Model Intercomparison Project (CMIP5) [*Taylor et al.*, 2012] for the Fifth Assessment Report (AR5) of the Inter Governmental Panel on Climate Change (IPCC), aim to provide understanding of potential climate change given scenarios of human economic and agricultural activity. The Representative Concentration Pathways (RCPs) [*van Vuuren et al.*, 2011] prescribe the amounts of anthropogenic emissions and land use change used by Earth System Models (ESMs) to estimate atmospheric CO_2 concentration and climate change (IPCC, 2013). Recent advances have improved communication between these modeling communities through dataset harmonization for common and consistent anthropogenic forcing of ESMs [*Hurtt et al.*, 2011; *Lamarque et al.*, 2010; *van Vuuren et al.*, 2011]. However, land use change is uniquely implemented in each ESM with differences in land cover representation, definitions, conversion processes, and assumptions [*Brovkin et al.*, 2013; *Pitman et al.*, 2009]. Furthermore, although land *use* was harmonized for CMIP5 [*Hurtt et al.*, 2011], each ESM used its own land *cover* distribution and conversion approach because the ESMs were structured to apply *exogenous land use* to *endogenous land cover* implementations. As Land Use and Land Cover Change (LULCC) has both biophysical [e.g., *Brovkin et al.*, 2013; *A D Jones et al.*, 2013a; *Pitman et al.*, 2009] and biogeochemical [e.g. *Arora and Boer*, 2010; *Di Vittorio et al.*, 2014; *Jain and Yang*, 2005; *Ying-Ping et al.*, 2015; *Zhang et al.*, 2013] effects on the Earth system, different implementations of the same land use scenario can constitute vastly different ESM LULCC scenarios, with corresponding differences in regional and global carbon [e.g., *Di Vittorio et al.*, 2014] and climate [e.g., *A D Jones et al.*, 2013a] projections.

The contribution of LULCC uncertainty to carbon and climate projections is important for understanding potential global change impacts, as many climate mitigation and adaptation strategies rely on local LULCC [e.g., *Rose et al.*, 2012; *S J Smith and Rothwell*, 2013; *van Vuuren et al.*, 2011] with corresponding effects on carbon [e.g., *Jain and Yang, 2005*] and climate [e.g., *Bright et al., 2017*]. Assessment of such strategies can be confounded if LULCC uncertainty is comparable to intra- or inter-scenario differences. For example, Peng et al. [2017] estimated a 1990 forest area uncertainty (2.9

Mkm^2) due to historical land conversion uncertainty that is ~161% of the estimated increase in RCP2.6 forest area from 2005 to 2100 and ~242% of the difference in estimated 2100 forest area between RCPs 2.6 and 6.0 [*Hurtt et al., 2011*]. The uncertainties in net LULCC emissions [*Ciais et al.*, 2013, Figure 6.10; *Houghton et al.*, 2012; *Le Quéré et al.*, 2015] and residual land-atmosphere CO_2 flux [*Ciais et al.*, 2013, Figure 6.16] are already large without accounting for land cover conversion uncertainty. Accounting for this uncertainty increases emissions uncertainty [*Peng et al.*, 2017] and affects the significance of land use strategies aiming to reduce emissions. Therefore, increasing accuracy and evaluation of LULCC, and in particular land cover change, is paramount for understanding global change.

Given the significant influence of LULCC on carbon and climate, a primary question remains largely unexplored: How large are uncertainties associated with the translation of land use change information into land cover change, in terms of global carbon and climate? A primary obstacle to exploring this question has been the limited LULCC flexibility in Earth system models [e.g., *Brovkin et al.*, 2013; *Pitman et al.*, 2009]. However, the integrated Earth System Model (iESM) [*Bond-Lamberty et al.*, 2014; *Collins et al.*, 2015; *Di Vittorio et al.*, 2014; *A D Jones et al.*, 2013a; *Thornton et al.*, 2017] provides a unique structure for addressing this question. Here, we use this model to quantify the envelope of uncertainties associated with land conversion assumptions and their effects on the global carbon-climate system during 1850-2004. We compare these uncertainties to those of CO_2 fertilization, climate change, and nitrogen deposition, and also analyze effects on local climate.

2 Materials and Methods

2.1 The integrated Earth System Model (iESM)

The iESM [*Bond-Lamberty et al.*, 2014; *Collins et al.*, 2015; *Di Vittorio et al.*, 2014; *A D Jones et al.*, 2013a; *Thornton et al.*, 2017] integrates the Global Change Assessment Model (GCAM, v3.0) [*Calvin et al.*, 2011], Global Land-use Model (GLM) [*Hurtt et al.*, 2011], and Community Earth System Model (CESM, v1.1.2) [*CESM1.1 Series Public Release*] following the CMIP5 land use harmonization protocol [*Hurtt et al.*, 2011] with additional feedbacks from the land surface in CESM to GCAM. A unique feature of the iESM is its inline Land Use Translator (LUT) that converts GLM outputs to CESM inputs [*Di Vittorio et al.*, 2014; *P Lawrence et al.*, 2012]. Here we use historical land use data from GLM [*Hurtt et al.*, 2011], and thus GCAM and GLM components are inactive. The initial conditions are from a standard year-1850 spinup simulation.

The iESM translates GLM land use change into iESM land cover change each year using an LUT with adjustable land cover conversion assumptions [*Di Vittorio et al.*, 2014; *P Lawrence et al.*, 2012]. Historical land use is provided globally at half degree grid cell fractional resolution, and includes cropland, pasture, urban, secondary and primary vegetation, annual transitions between these categories, and both area and amounts of wood harvest [*Hurtt et al.*, 2011]. The LUT uses only annual crop and pasture and harvested area information to coincide with iESM land model implementation (Community Land Model v4, CLM) [*D M Lawrence et al.*, 2011]. Given user-specified land cover conversion assumptions, the LUT converts GLM land use change to changes in CLM land cover, which lacks pasture and comprises 16 Plant Functional Types (PFTs): bare ground, eight trees, three grasses, three shrubs, and one crop. The initial GLM pasture area is assigned first to grass PFTs, then to shrubs, and finally to trees, as needed. All new pasture is added as grass. A unique feature of the LUT is that it can track existing pasture in relation to CLM PFTs throughout a simulation. The LUT can be configured with different reference years for calculating LULCC and with land cover conversion assumptions ranging continuously between maximizing and minimizing forest area. There are separate parameters for expansion and contraction of agriculture, and each of these parameters defines the relative amounts of forest versus grass/shrub PFTs to convert. The center of this assumption range converts land cover proportionally to existing (for agricultural expansion) or potential (for agricultural contraction) PFT coverage.

2.2 Historical LULCC simulations

2.2.1 Land model only simulations

We performed eight, half-degree, global, land only simulations to separate the effects of LULCC and atmospheric inputs on carbon (Table 1). These simulations varied in reference year, land cover conversion assumptions, and atmospheric forcing. We used two standard LULCC configurations and designed three more to span a maximum range of land cover conversion. These configurations are based on different reference years and land cover conversion assumptions, but with identical land use data and the same initial PFT distribution in 1850. “No LULCC” with no wood harvest is a standard reference configuration for estimating net LULCC emissions and ecosystem carbon changes due to LULCC. These estimates are based on the difference between another simulation and this No LULCC case, with net emissions constituted by net ecosystem exchange minus wildfire emissions. The “Default” case is the standard LULCC configuration for CESM, and it uses year 2000 as the reference for calculating each year’s land use/cover distribution [*P Lawrence et al.*, 2012]. The three other LULCC configurations use the previous year for reference (chronological), and are used to quantify maximum uncertainty ranges associated with land cover conversion: “Max Forest” preferentially converts grass and shrubs upon agricultural expansion and expands forest to its potential limit upon agricultural contraction, “Min Forest” preferentially converts forest upon agricultural expansion and expands grass and shrubs to their potential limits upon agricultural contraction, and “Proportional” removes or adds PFT area proportionally to existing or potential PFT coverage for agricultural expansion and contraction, respectively. These three chronological LULCC configurations also account for existing pasture when calculating PFT distribution, which means that new cropland or pasture cannot replace PFTs that are already assigned to pasture. In addition to the simulations corresponding to the LULCC configurations, we ran three Proportional simulations with specific atmospheric forcings held constant. These constant forcing simulations are used to quantify the effects of CO_2, climate, and N deposition on the terrestrial carbon budget. Two additional, intermediate LULCC configurations are presented in Text S1.

We used the land use change module [*P J Lawrence et al.*, 2012] with carbon-nitrogen biogeochemistry [*Thornton et al.*, 2007] for all cases. The CRU-NCEP data [*CRU-NCEP data*] were the meteorological drivers and years 1901-1920 were cycled prior to 1901. The "Constant climate and CO_2" case continued to cycle these years after 1920. The simulations also used transient CO_2 and aerosol concentrations and nitrogen deposition, following CMIP5 protocols, except for constant forcing cases. The "Constant climate and CO_2" and "Constant CO_2" cases held CO_2 concentration at the 1850 level, and the "Constant N deposition" case held nitrogen deposition at the 1850 level.

2.2.2 Coupled Earth system model simulations

We performed four, one-degree (0.9375°x1.25°), fully coupled simulations that were otherwise identical to their corresponding land model only simulations (Table 1). The additional active components were a dynamic ocean [*R Smith et al.*, 2013], the Community Atmosphere Model v5 [*Neale et al.*, 2012], and prognostic land-atmosphere-ocean biogeochemistry. We also used the CMIP5 historical CO_2, aerosol, and reactive gas emissions forcings [*Lamarque et al.*, 2010, *Meinshausen et al.*, 2011].

3 Results

3.1 Global carbon cycle

Forest area is a primary driver of global carbon uncertainty due to land cover conversion assumptions. Shifting from a year-2000 reference to chronological LULCC and accounting for existing pasture reduces forest and shrub areas and increases grass area because additional pasture requires land to be cleared (Figure 1). This causes the chronological cases to deviate from the Default PFT distribution by 2005, with a 5.1 M km^2 difference in forest area between the Max and Min Forest cases, mostly compensated for by grass. Also, the Max Forest case has a similar global forest area trajectory to the Default case, with a final value of ~42 M km^2. The one-degree, fully coupled simulations have nearly identical PFT distributions to the half-degree simulations, with the exception of the Max Forest case having ~1 M km^2 less forest and more grass by 2005 due to resolution-dependent limits to adding forest area. This results in a 3.9 M km^2 difference in forest area between the Max and Min Forest cases for the fully coupled analyses.

The land-only, chronological cases enable us to directly quantify and compare the effects of land cover conversion uncertainty, CO_2 concentration, climate, and nitrogen deposition on net LULCC emissions. Land cover change leading to a final forest area difference of 5.1 M km^2 constitutes uncertainty in the global carbon cycle comparable to the combined effects of CO_2 concentration and climate on LULCC carbon emissions, and greater than those of nitrogen deposition. The chronological cases generally have higher net direct annual LULCC emissions than the Default, and the annual CO_2 and nitrogen deposition effects do not exceed the Max to Min Forest range until after 1950 (Figure 2). Cumulatively, the 59 PgC Max to Min Forest range of emissions from 1850-2004 is greater than the individual effects of increasing CO_2 (-55 PgC) and nitrogen deposition (-27 PgC). Climate change has a negligible effect on the cumulative emissions (+2 PgC). For comparison, the range between Min Forest and Default for years 1850-1990 is 61 PgC, which is less than the overall range of 98 PgC reported by Peng et al. [2017] that includes methodological and data uncertainty in addition to land cover conversion uncertainty. With respect to emissions estimates, the Max Forest case has 190 PgC of cumulative emissions, which is within the 110-210 range presented by Smith and Rothwell (2013). Our uncertainty range is 37% of their midpoint value and the Min Forest case (249 PgC) exceeds their range.

Land cover conversion uncertainty also generates large uncertainty in land and atmosphere carbon stocks. The 33 PgC Max to Min Forest range of terrestrial ecosystem carbon lost to LULCC by 2005 is 80% of the corresponding net effects of increasing CO_2 plus climate change (41 PgC) (Figure 2). As expected, the intermediate cases give intermediate results with an ecosystem carbon range that is 46% of this net CO_2 plus climate effect (Text S1 and Figure S2). Also as expected, the regional distribution of this uncertainty depends on forest difference (Figure 3a) and carbon content (Figure S3). Climate change increases terrestrial carbon loss by 11 PgC, likely through reduction of productivity on abandoned land, while CO_2 and nitrogen deposition decrease loss by 52 and 27 PgC, respectively, likely due to fertilization effects. Based on the fully coupled simulations, the Proportional case increases the 15 ppmv Default case bias in atmospheric CO_2 to 21 ppmv, and the Max to Min Forest range is 5 ppmv. The Max Forest case has similar global forest area to the Default case, but an additional 9 PgC of carbon is lost in the Max Forest case due to shrub loss, increasing the atmospheric bias to 20 ppmv. These differences in ecosystem carbon and CO_2 concentration are compensated by differences in ocean carbon, with 40% and 49% of additional ecosystem carbon loss going to the ocean for Max Forest versus Default and Min Forest, respectively.

3.2 Local climate

Earth system model simulations demonstrate that relatively small uncertainties in land cover lead to significant differences in regional climate through biophysical effects. The Max minus Min Forest difference in forest cover ranges from -8 to 31 percent of the grid cell, with per cell surface temperature differences ranging from -0.87 to 1.62 °C (Figures 3, S4). These values are greater than the LULCC effects on land surface temperature for RCPs 2.6 and 8.5 estimated by Brovkin et al. [2013]. Our per-cell uncertainty range for June-July-August is -0.75 to 1.37 °C, which is comparable to historical LULCC effects on land surface temperature estimated by Pitman et al. [2009]. While albedo generally decreases with increasing tree cover, thus increasing shortwave radiation absorbed by the surface, the local surface temperature both increases and decreases with increasing tree cover due to compensating effects of latent and sensible heating. Sensible heating is more sensitive than latent heating to changes in forest cover at the grid cell level (Figure S5), which contributes to the Max Forest case having a global average temperature (1985-2004) that is 0.1 °C greater than that of the Min Forest case.

4 Discussion

Land cover conversion assumptions and uncertainties significantly affect carbon and climate projections. These uncertainties drive global carbon cycle uncertainty that is comparable to the net effects of CO_2 and climate on the global carbon cycle from 1850 to 2004, and greater than the effects of nitrogen deposition. Climate change has little effect on net LULCC emissions, but it does increase the amount of terrestrial carbon lost to LULCC. Relatively small differences (<10% of grid cell) in forest cover can generate differences in local surface temperature of over 1 °C, which is comparable to estimated effects of LULCC on temperature [Brovkin et al., 2013; Pitman et al., 2009]. This temperature uncertainty is regionally dependent and the sign varies in response to local and distributed effects of land cover change, combined with differences in the general circulation associated with different land surface trajectories. Our results are conservative, in that we focus on uncertainty in land cover conversion assumptions. Additional sources of uncertainty include the land use forcing data, the initial and present-day land distributions, and model implementation of LULCC.

Our results suggest that the initial, transient, and final CLM land cover distributions may not reflect actual distributions. Basing LULCC on changes from the previous year and accounting for existing pasture moves the iESM farther from current land cover and carbon cycle estimates, and requires forest maximization assumptions to bring it back to default CESM carbon cycle behavior. However, it is unlikely that a single conversion assumption adequately represents the entire globe [Prestele et al., 2017]. Nonetheless, the extreme assumptions in this study are not far from other assumptions used in ESMs [Peng et al., 2017; Prestele et al., 2017], and reliably represent a maximum uncertainty envelope. Developing more realistic conversion assumptions will require further exploration of LULCC methods and initial and final states.

The final global forest area of the chronological cases is more consistent with estimates from other land cover studies, although still high, depending on forest definition. In the iESM forest area is based on PFTs, which correspond more directly with tree cover than with a broad range of forest canopy cover. In a PFT-focused effort, Meiyappan and Jain [2012] use the International Geosphere-Biosphere Programme (IGBP) definition of forest (>60% tree cover) and a spatial-coherence method for splitting mixed forest pixels. They also use three different land use data sources, and estimate 2005 global forest area between 28.1 and 30 M km^2, which is over 7 M km^2 less than the 37.0 M km^2 in our “Min Forest” case. Their 7.1-14.2 M km^2 estimate of savanna refers to tropical grassland, which would not make up the difference in forest area, as the IGBP definitions of savanna (10-30% tree cover) and woody savanna (30-60% tree cover) do not have enough trees [*M. A. Friedl et al.*, 2002]. Similarly, Friedl et al. [2010] estimate 28.4 M km^2 of forest area (>60% tree cover), 13.6 M km^2 of woody savanna, 8.6 M km^2 of savanna, 2.5 M km^2 of closed shrublands (>60% shrub cover), 20.2 M km^2 of open shrublands (10-60% shrub cover), and 15.2 M km^2 of grassland in the early 2000s. The iESM’s shrub (~10 M km^2) and grass (28.6-33.5 M km^2) estimates are consistent with these estimates, especially considering that PFTs represent specific vegetation cover while land cover classes, including pasture, incorporate multiple vegetation types. However, this comparison is limited because iESM assigns initial pasture to various PFTs and assumes that all new pasture is grass. Alternatively, Sexton et al. [2016] report a wide range of year-2000 forest area based on Landsat data and three different tree cover thresholds: 51.5 M km2 (>10%), 32.2 M km2 (>30%), and 16.1 M km2 (>60%). Clearly, these examples demonstrate considerable variability across estimates of present day land cover, which implies similar or greater variability in historical LULCC trajectories. Furthermore, a recent study shows that uncertainty in present day land cover contributes substantial uncertainty to albedo, evapotranspiration, and gross primary productivity in three land surface models [Hartley et al., in press], and variability across LULCC trajectories directly contributes to high variability across terrestrial carbon estimates [*Di Vittorio et al.*, 2014]. This indicates that assuming a single LULCC trajectory for global modeling and analysis ignores considerable uncertainty that can have dramatic effects on carbon and climate projections.

The estimated effects of land cover uncertainty on temperature include local and regionally distributed effects of LULCC in addition to changes in general circulation due to different land surface states. While new methods aim to isolate the local effects of LULCC in model outputs to improve understanding and comparisons with observations [*Lejeune et al.*, 2017; *Winckler et al.*, 2017], model uncertainty quantification needs to include all relevant components in order to capture the entire error range associated with projections. In this context, increases in forest cover drive regionally dependent increases or decreases in temperature, even in places with no difference in forest cover (Figures 3, S4). This is consistent with Swann et al. [2012], who report that large differences in forest area could shift general circulation patterns, affecting both precipitation and temperature beyond the extent of forest cover change. Furthermore, our results include changes in general circulation influenced by ocean responses to differences in land cover.

As such, our uncertainty estimates are comprehensive with respect to fully coupled climate projections that provide inputs to impact analyses, which rely heavily on local and regional estimates [*Field et al.*, 2014]. Overall, land cover conversion uncertainty is a substantial and important component of local climate uncertainty that becomes even more critical when augmented by the related data and methodological uncertainties discussed above.

These results demonstrate the importance of accurate LULCC implementation and reliable LULCC uncertainty characterization when assessing climate mitigation and adaptation strategies and impacts through scenario-based modeling. LULCC uncertainty can completely change the location and type of prescribed land conversion, which affects local to global carbon and climate. For example, our final forest area uncertainty is 61% of the 8.3 M km^2 of forest lost from 2005-2100 in RCP8.5 and 78% of the 6.5 M km^2 of forest gained in RCP4.5 [*Hurtt et al.*, 2011; Fig. 9]. Given the variability in land implementation among ESMs [*Brovkin et al.*, 2013] and the resulting potential range of effects [e.g., *Di Vittorio et al.*, 2014], LULCC uncertainty significantly contributes to model disagreement within an RCP. For land carbon projections in particular, LULCC uncertainty plays a central role in keeping the RCPs from diverging [*C Jones et al.*, 2013b; Figures 2 and 3] when they should represent differences in land-based climate mitigation strategies. While other factors also contribute to model disagreement and scenario overlap, evaluation of climate mitigation and adaptation strategies is not possible if different scenarios are not distinguishable from each other.

We conclude that improving LULCC characterization and implementation can increase understanding and improve carbon and climate projections. Current efforts include adding forest area to CMIP6 land use scenarios (http://www.geosci-model-dev-discuss.net/gmd-2016-76/). Such efforts facilitate a needed increase in consistency, accuracy, and uncertainty characterization of land cover data and implementation across models. Overall, it is critical to integrate land use and land cover analysis to provide better initial, transient, present-day, and future land use and land cover distributions, improve implementations of LULCC in earth system models, and enable models to be more faithful to historical and projected LULCC.

Acknowledgments

This work is supported by the US Department of Energy, Office of Science, Office of Biological and Environmental Research under Award Number DE-AC02-05CH11231 as part of the Integrated Assessment Research and Earth System Modeling Programs and with additional support from the Accelerated Climate Modeling for Energy project. J.Mao and X.Shi are also supported by the Biogeochemistry-Climate Feedbacks Scientific Focus Area project funded through the Regional and Global Climate Modeling Program in the Climate and Environmental Sciences Division (CESD) of the Biological and Environmental Research (BER) Program in the US Department of Energy Office of Science. G. Hurtt and L. Chini gratefully acknowledge the support of NASA-IDS and DOE-SciDAC programs. Oak Ridge National Laboratory is managed by UT-BATTELLE for DOE under contract DE-AC05-00OR22725. project used resources of the National

Energy Research Scientific Computing Center (NERSC), which is a DOE Office of Science user Facility. The CESM project is supported by the National Science Foundation and the Office of Science (Biological and Environmental Research) of the US Department of Energy. The authors also acknowledge high-performance computing support from Yellowstone (ark:/85065/d7wd3xhc) provided by NCAR's Computational and Information Sytems Laboratory, sponsored by the National Science Foundation. The authors are grateful to Ben Bond-Lamberty and reviewers for providing insightful feedback on drafts of this manuscript.

The authors declare that there are no real or perceived financial conflicts of interest.

Data

Model outputs corresponding with the figures are included as supplemental information, and the raw model outputs will be archived for at least five years from publication. Please contact the corresponding author to obtain access to the raw model outputs. The iESM code is available at https://github.com/ACME-Climate/iESM. On the Yellowstone supercomputing cluster, the 8 land-only simulations used about 224,000 processor hours each, and two of the fully coupled simulations used about 700,000 processor hours each. The other two fully coupled simulations used about 1.5 M processor hours each on the Edison supercomputing cluster at NERSC, and were charged twice this amount due to a 2X charge factor.

References

Arora, V. K., and G. J. Boer (2010), Uncertainties in the 20th century carbon budget associated with land use change, *Global Change Biol.*, *16*(12), 3327-3348, doi:10.1111/j.1365-2486.2010.02202.x.

Bond-Lamberty, B., K. Calvin, A. D. Jones, J. Mao, P. Patel, X. Y. Shi, A. Thomson, P. Thornton, and Y. Zhou (2014), On linking an Earth system model to the equilibrium carbon representation of an economically optimizing land use model, *Geosci. Model Dev.*, *7*(6), 2545-2555, doi:10.5194/gmd-7-2545-2014.

Bright, R. M., E. Davin, T. O/'Halloran, J. Pongratz, K. Zhao, and A. Cescatti (2017), Local temperature response to land cover and management change driven by non-radiative processes, *Nature Clim. Change*, *7*(4), 296-302, doi:10.1038/nclimate3250
http://www.nature.com/nclimate/journal/v7/n4/abs/nclimate3250.html#supplementary-information.

Brovkin, V., et al. (2013), Effect of Anthropogenic Land-Use and Land-Cover Changes on Climate and Land Carbon Storage in CMIP5 Projections for the Twenty-First Century, *J. Clim.*, *26*(18), 6859-6881, doi:10.1175/jcli-d-12-00623.1.

CESM 1.1 Series Public Release available at: http://www.cesm.ucar.edu/models/cesm1.1/; last access: 13 July 2017.

Ciais, P., C. Sabine, G. Bala, L. Bopp, V. Brovkin, J. Canadell, A. Chhabra, R. DeFries, J. Galloway, M. Heimann, C. Jones, C. Le Quéré, R.B. Myneni, S. Piao and P. Thornton, 2013: Carbon and Other Biogeochemical Cycles. In: *Climate Change*

2013: The Physical Science Basis. Contribution of Working Group I to the Fifth Assessment Report of the Intergovernmental Panel on Climate Change [Stocker, T.F., D. Qin, G.-K. Plattner, M. Tignor, S.K. Allen, J. Boschung, A. Nauels, Y. Xia, V. Bex and P.M. Midgley (eds.)]. Cambridge University Press, Cambridge, United Kingdom and New York, NY, USA.

Collins, W. D., et al. (2015), The integrated Earth system model version 1: formulation and functionality, *Geosci. Model Dev.*, *8*(7), 2203-2219, doi:10.5194/gmd-8-2203-2015.

CRU-NCEP data available at: https://www.earthsystemgrid.org/dataset/ucar.cgd.ccsm4.CRUNCEP.v4.html; last access: 13 July 2017.

Di Vittorio, A. V., et al. (2014), From land use to land cover: restoring the afforestation signal in a coupled integrated assessment-earth system model and the implications for CMIP5 RCP simulations, *Biogeosciences*, *11*(22), 6435-6450, doi:10.5194/bg-11-6435-2014.

Field, C.B., et al. (2014), Technical summary. In: *Climate Change 2014: Impacts, Adaptation, and Vulnerability. Part A: Global and Sectoral Aspects. Contribution of Working Group II to the Fifth Assessment Report of the Intergovernmental Panel on Climate Change* [Field, C.B., et al. (eds.)]. Cambridge University Press, Cambridge, United Kingdom and New York, NY, USA, pp. 35-94.

Friedl, M. A., et al. (2002), Global land cover mapping from MODIS: algorithms and early results, *Remote Sens. Environ.*, *83*(1–2), 287-302, doi: 10.1016/S0034-4257(02)00078-0.

Friedl, M. A., D. Sulla-Menashe, B. Tan, A. Schneider, N. Ramankutty, A. Sibley, and X. Huang (2010), MODIS Collection 5 global land cover: Algorithm refinements and characterization of new datasets, *Remote Sens. Environ.*, *114*(1), 168-182, doi: 10.1016/j.rse.2009.08.016.

Hartley, A. J., N. MacBean, G. Georgievski, and S. Bontemps (in press), Unceratinty in plant functional type distributions and its implications on land surface models, *Remote Sens. Environ.*, doi: 10.1016/j.rse.2017.07.037.

Houghton, R. A., J. I. House, J. Pongratz, G. R. van der Werf, R. S. DeFries, M. C. Hansen, C. Le Quere, and N. Ramankutty (2012), Carbon emissions from land use and land-cover change, *Biogeosciences*, *9*(12), 5125-5142, doi:10.5194/bg-9-5125-2012.

Hurtt, G. C., et al. (2011), Harmonization of land-use scenarios for the period 1500-2100: 600 years of global gridded annual land-use transitions, wood harvest, and resulting secondary lands, *Clim. Change*, *109*(1-2), 117-161, doi:10.1007/s10584-011-0153-2.

IPCC, 2013: Summary for Policymakers. In: *Climate Change 2013: The Physical Science Basis. Contribution of Working Group I to the Fifth Assessment Report of the Intergovernmental Panel on Climate Change* [Stocker, T.F., D. Qin, G.-K. Plattner, M. Tignor, S.K. Allen, J. Boschung, A. Nauels, Y. Xia, V. Bex and P.M. Midgley (eds.)]. Cambridge University Press, Cambridge, United Kingdom and New York, NY, USA.

Jain, A. K., and X. Yang (2005), Modeling the effects of two different land cover change data sets on the carbon stocks of plants and soils in concert with CO_2 and climate change, *Global Biogeochemical Cycles*, *19*(2), GB2015, doi:10.1029/2004gb002349.

Jones, A. D., et al. (2013a), Greenhouse Gas Policy Influences Climate via Direct Effects of Land-Use Change, *J. Clim.*, *26*(11), 3657-3670, doi:10.1175/jcli-d-12-00377.1.

Jones, C., et al. (2013b), Twenty-First-Century Compatible CO_2 Emissions and Airborne Fraction Simulated by CMIP5 Earth System Models under Four Representative Concentration Pathways, *J. Clim.*, *26*(13), 4398-4413, doi:10.1175/jcli-d-12-00554.1.

Lamarque, J. F., et al. (2010), Historical (1850–2000) gridded anthropogenic and biomass burning emissions of reactive gases and aerosols: methodology and application, *Atmos. Chem. Phys.*, *10*(15), 7017-7039, doi:10.5194/acp-10-7017-2010.

Lawrence, D. M., et al. (2011), Parameterization improvements and functional and structural advances in Version 4 of the Community Land Model, *Journal of Advances in Modeling Earth Systems*, *3*(3), M03001, doi:10.1029/2011ms000045.

Lawrence, P. J., et al. (2012), Simulating the Biogeochemical and Biogeophysical Impacts of Transient Land Cover Change and Wood Harvest in the Community Climate System Model (CCSM4) from 1850 to 2100, *J. Clim.*, *25*(9), 3071-3095, doi:10.1175/jcli-d-11-00256.1.

Le Quéré, C., et al. (2015), Global carbon budget 2014, *Earth Syst. Sci. Data*, *7*(1), 47-85, doi:10.5194/essd-7-47-2015.

Lejeune, Q., S. I. Seneviratne, and E. L. Davin (2017), Historical Land-Cover Change Impacts on Climate: Comparative Assessment of LUCID and CMIP5 Multimodel Experiments, *J. Clim.*, *30*(4), 1439-1459, doi:10.1175/jcli-d-16-0213.1.

Meinshausen, M., S. J. Smith, K. Calvin, J. S. Daniel, M. L. T. Kainuma, J-F Lamarque, K. Matsumoto, S. A. Montzka, S. C. B. Raper, K. Riahi, A. Thomson, G. J. M. Velders, D. P. P. van Vuuren (2011), The RCP greenhouse gas concentrations and their extensions from 1765 to 2300, Climatic Change, 109, 213-241, doi: 10.1007/s10584-011-0156-z.

Meiyappan, P., and A. Jain (2012), Three distinct global estimates of historical land-cover change and land-use conversions for over 200 years, *Front. Earth Sci.*, *6*(2), 122-139, doi:10.1007/s11707-012-0314-2.

Neale, R.B., A. Gettleman, S. Park, C.-C. Chen, P.H. Lauritzen, D.L. Williamson, A.J. Conley, D. Kinnison, D. Marsh, A.K. Smith, F. Vitt, R. Garcia, J.-F. Lamarque, M. Mills, S. Tilmes, H. Morrrison, P. Cameron –Smith, W.D. Collins, M.J. Iacono, R.C. Easter, X. Liu, S.J. Ghan, R.J. Rasch, and M.A. Taylor (2012), Description of the NCAR Community Atmosphere Model (CAM 5.0), NCAR/TN-486+STR, NCAR, Boulder, CO, USA.

Peng, S., P. Ciais, F. Maignan, W. Li, J. Chang, T. Wang, and C. Yue (2017), Sensitivity of land use change emission estimates to historical land use and land cover mapping, *Global Biogeochemical Cycles*, *31*(4), 2015GB005360, doi:10.1002/2015GB005360.

Pitman, A. J., et al. (2009), Uncertainties in climate responses to past land cover change: First results from the LUCID intercomparison study, *Geophys. Res. Lett.*, *36*(14), L14814, doi:10.1029/2009gl039076.

Prestele, R., A. Arneth, A. Bondeau, N. de Noblety-Ducoudre, T. A. M. Pugh, S. Sitch, E. Stehfest, and P. Verburg (2017), Current challenges of implementing anthropogenic land-use and land-cover change in models contributing to climate change assessments, Earth System Dynamics, 8, 369-386, doi: 10.5194/esd-8-369-2017.

Rose, S. K., H. Ahammad, B. Eickhout, B. Fisher, A. Kurosawa, S. Rao, K. Riahi, and D. P. van Vuuren (2012), Land-based mitigation in climate stabilization, *Energy Economics*, *34*(1), 365-380, doi: 10.1016/j.eneco.2011.06.004.

Sexton, J. O., P. Noojipady, X.-P. Song, M. Feng, D.-X. Song, D.-H. Kim, A. Anand, C. Huang, S. Channan, S. L. Pimm, and J. R. Townshend (2016), Conservation policy and the measurement of forests, Nature Climate Change, 6(2), 192-196, doi: 10.1038/NCLIMATE2816.

Smith, R., et al. (2013), The Parallel Ocean Program (POP) reference manual*Rep.*, 183 pp, Los Alamos National Laboratory.

Smith, S. J., and A. Rothwell (2013), Carbon density and anthropogenic land-use influences on net land-use change emissions, *Biogeosciences*, *10*(10), 6323-6337, doi:10.5194/bg-10-6323-2013.

Swann, A. L. S., I. Y. Fung, and J. C. H. Chiang (2012), Mid-latitude afforestation shifts general circulation and tropical precipitation, *Proceedings of the National Academy of Sciences*, *109*(3), 712-716, doi:10.1073/pnas.1116706108.

Taylor, K. E., R. J. Stouffer, and G. A. Meehl (2012), An Overview of CMIP5 and the Experiment Design, *Bulletin of the American Meteorological Society*, *93*(4), 485-498, doi:10.1175/bams-d-11-00094.1.

Thornton, P. E., J.-F. Lamarque, N. A. Rosenbloom, and N. M. Mahowald (2007), Influence of carbon-nitrogen cycle coupling on land model response to CO2 fertilization and climate variability, *Global Biogeochemical Cycles*, *21*(4), GB4018, doi:10.1029/2006gb002868.

Thornton, P. E., Calvin, K., Calvin, K., Jones, A. D., Jones, A. D., Di Vittorio, A. V., et al. (2017). Biospheric feedback effects in a synchronously coupled model of human and Earth systems, *Nature Climate Change*, 119, 141–6, doi: 10.1038/nclimate3310.

Van Vuuren, D., et al. (2011), The representative concentration pathways: an overview, *Clim. Change*, *109*(1-2), 5-31, doi:10.1007/s10584-011-0148-z.

Winckler, J., C. H. Reick, and J. Pongratz (2017), Robust Identification of Local Biogeophysical Effects of Land-Cover Change in a Global Climate Model, *J. Clim.*, *30*(3), 1159-1176, doi:10.1175/jcli-d-16-0067.1.

Ying-Ping, W., Z. Qian, J. P. Andrew, and D. Yongjiu (2015), Nitrogen and phosphorous limitation reduces the effects of land use change on land carbon uptake or emission, *Environmental Research Letters*, *10*(1), 014001.

Zhang, Q., A. J. Pitman, Y. P. Wang, Y. J. Dai, and P. J. Lawrence (2013), The impact of nitrogen and phosphorous limitation on the estimated terrestrial carbon balance and warming of land use change over the last 156 yr, *Earth Syst. Dynam.*, *4*(2), 333-345, doi:10.5194/esd-4-333-2013.

Table 1. Eight half-degree land model simulations and four corresponding one-degree Earth system model (denoted by *) simulations (1850-2004). These are all transient simulations using CMIP5 protocols, except where a particular forcing is noted to be constant. The land change reference is the base year for calculating LULCC change to obtain each year's land use/cover distribution.

Case	**Land change reference**	**Land cover conversion assumptions**
No LULCC	Constant 1850	No land use, land cover conversion, or wood harvest
Default*	Year 2000	Changes in Plant Functional Types (PFTs) are proportional to current (removal) or potential (addition) PFT distribution
Max Forest*	Previous year	Changes in pasture/crop maximize forest area; accounts for existing pasture
Proportional*	Previous year	Changes in PFTs are proportional to current (removal) or potential (addition) PFT distribution; accounts for existing pasture
Min Forest*	Previous year	Changes in pasture/crop minimize forest area; accounts for existing pasture
Constant climate and CO_2	Previous year	Same as Proportional case
Constant CO_2	Previous year	Same as Proportional case
Constant N deposition	Previous year	Same as Proportional case

Figure Captions

Figure 1. Global plant functional type (PFT) areas for half-degree, land-only simulations in Table 1. The No LULCC case maintains 1850 areas through 2005 for all PFTs. Crop area is the same for all cases except No LULCC. These areas are nearly identical for the one-degree, fully coupled simulations, except that Max Forest has ~1 M km^2 less forest and more grass by 2005. The constant CO_2, climate, and N deposition cases have the same areas as the Proportional case.

Figure 2. Effects of Land Use and Land Cover Change (LULCC) uncertainty and atmospheric forcing on terrestrial carbon. Effects of a) land cover uncertainty and b) atmospheric forcing on net annual LULCC emissions. Effects of a) land cover uncertainty and b) atmospheric forcing on change in total ecosystem carbon due to LULCC. These results are from land-only simulations. Emission values are 11-year running averages of the difference between each LULCC case and the No LULCC case of: net ecosystem exchange minus natural fire emissions. Ecosystem carbon values are the differences between each LULCC case and the No LULCC case.

Figure 3. Regional patterns of a) differences in forest cover and b) differences in surface air temperature. These values are differences between 20-year annual averages (1985-2004, Max Forest minus Min Forest).

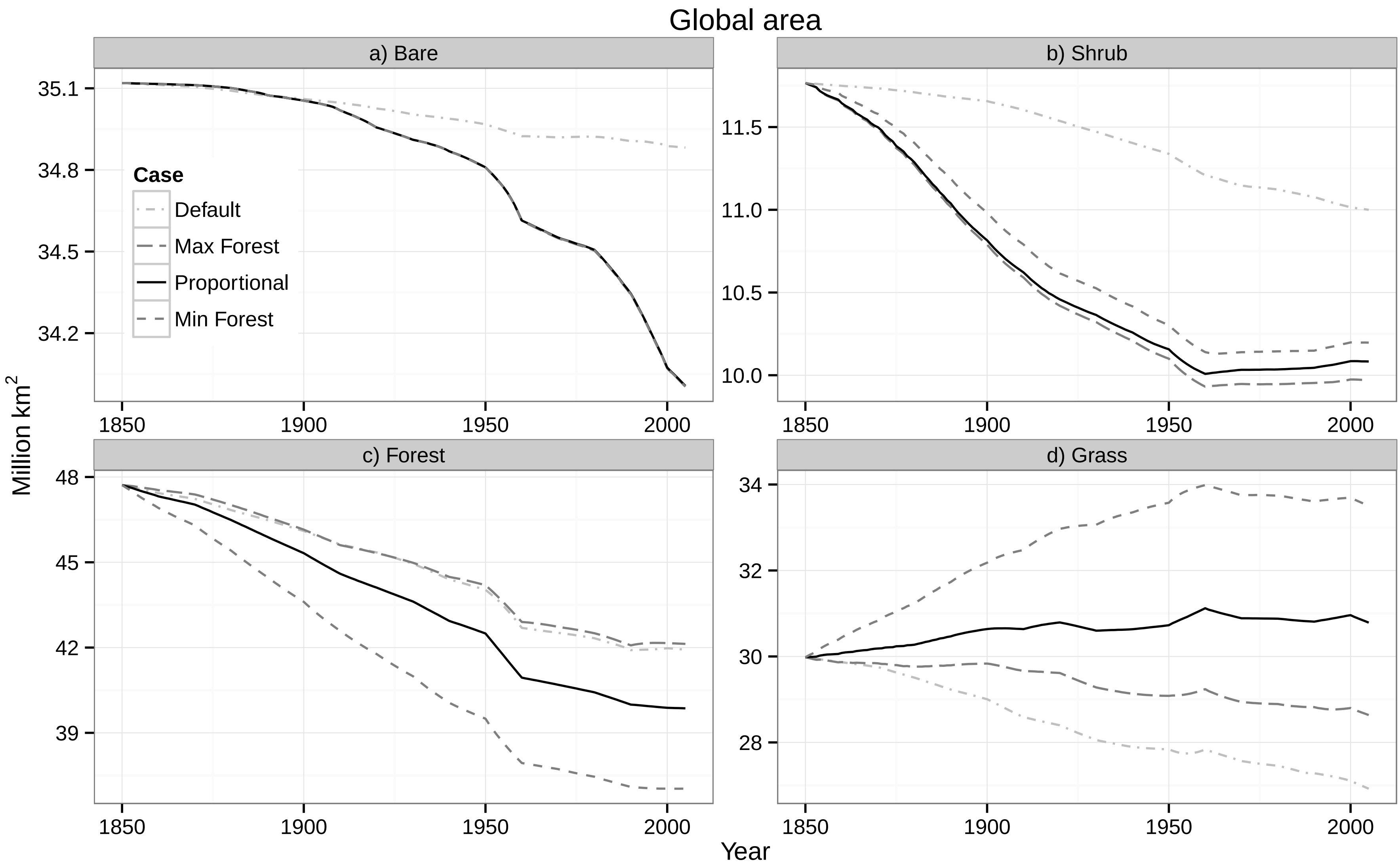

Global area
a) Bare
b) Shrub
c) Forest
d) Grass
Case
Default
Max Forest
Proportional
Min Forest
Million km2
Year
35.1
34.8
34.5
34.2
11.5
11.0
10.5
10.0
48
45
42
39
34
32
30
28
1850
1900
1950
2000

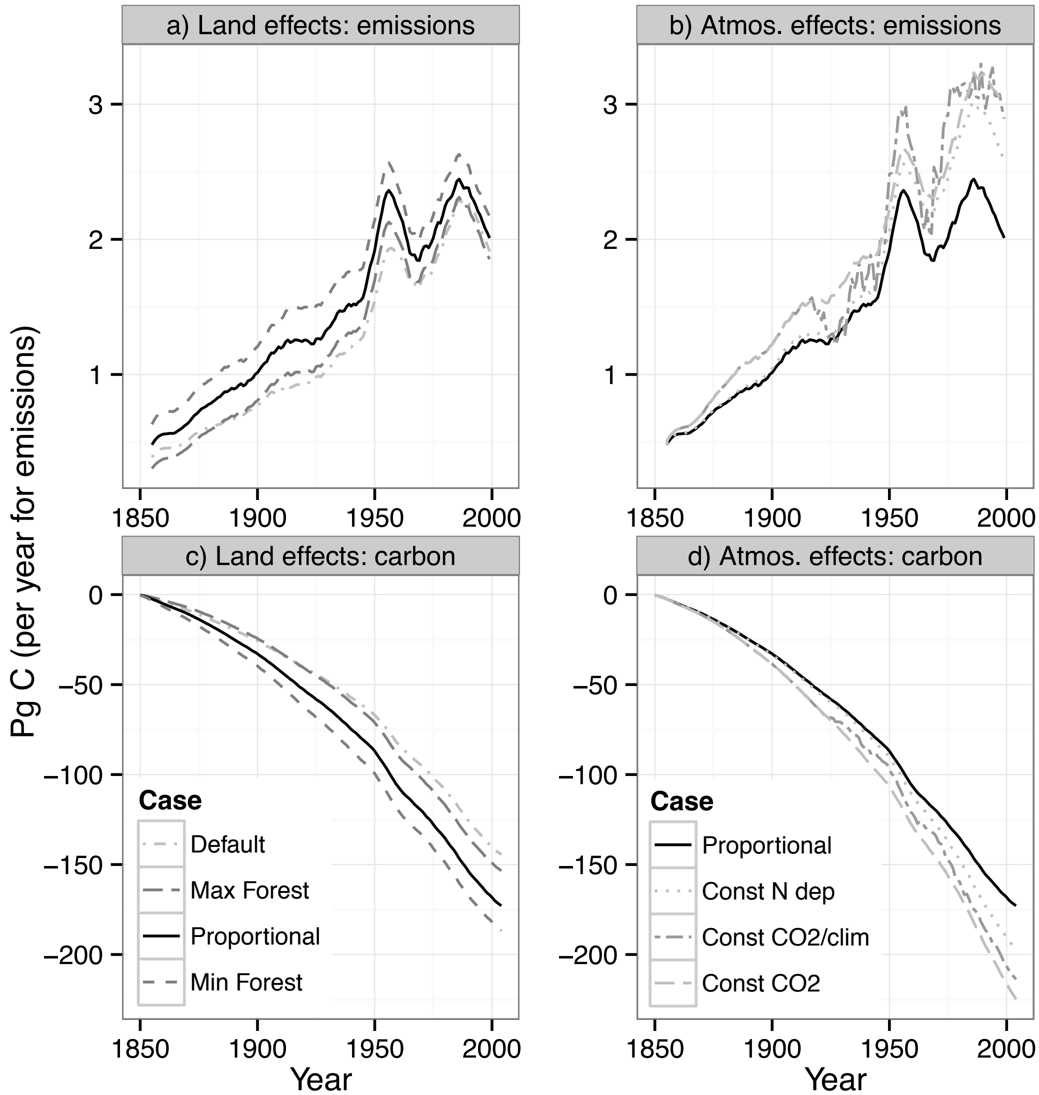
a) Land effects: emissions
b) Atmos. effects: emissions
c) Land effects: carbon
d) Atmos. effects: carbon
Pg C (per year for emissions)
Year
Case
Default
Max Forest
Proportional
Min Forest
Case
Proportional
Const N dep
Const CO2/clim
Const CO2

a) Forest cover difference, Max Forest minus Min Forest (% of grid cell)

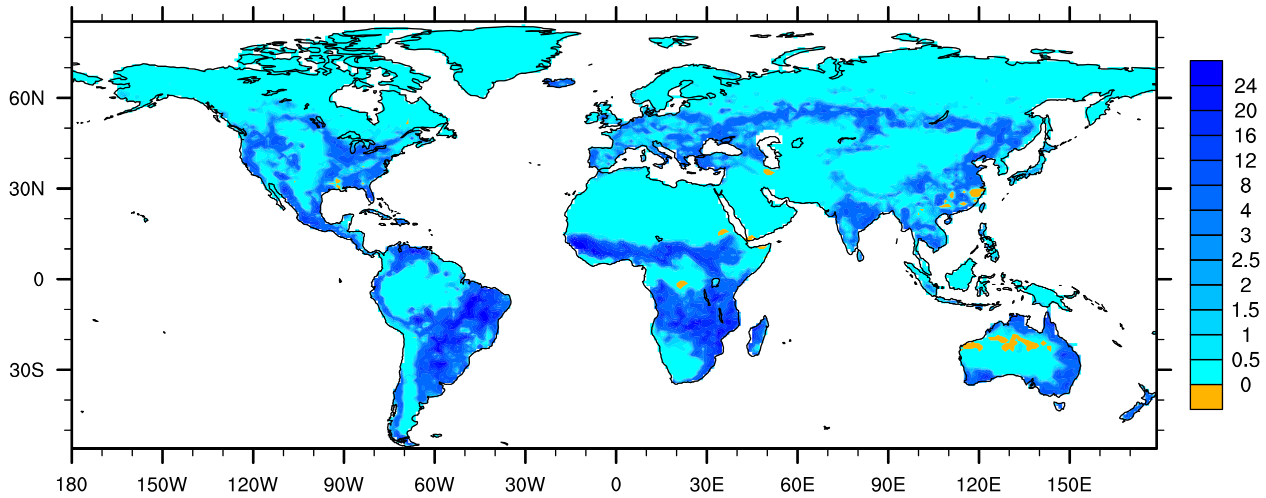

b) Surface air temperature difference, Max Forest minus Min Forest (°C)

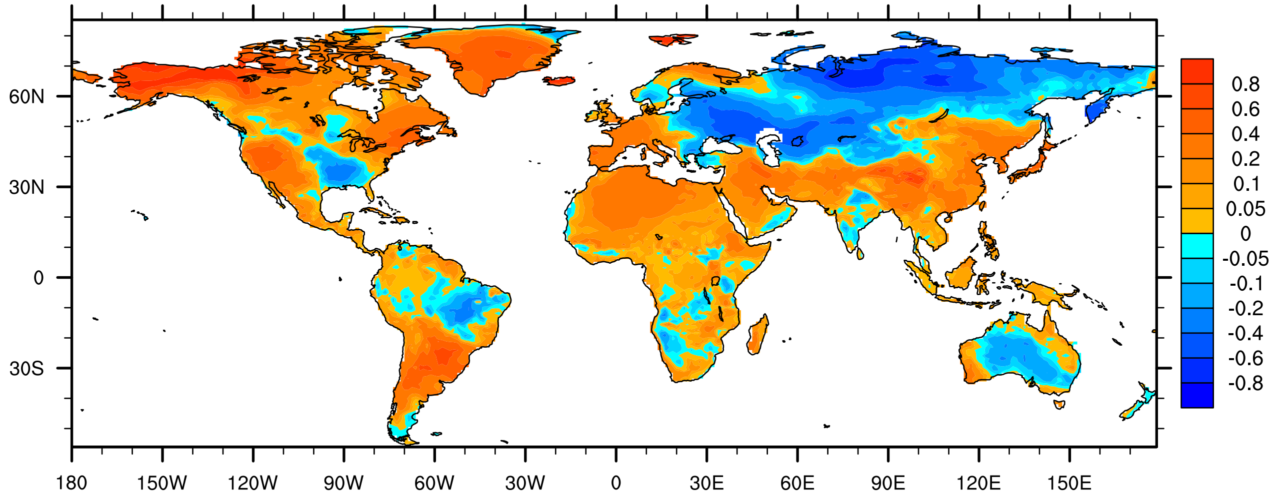

Geophysical Research Letters

Supporting Information for

Land cover uncertainty has a substantial effect on carbon and climate projections

A. V. Di Vittorio[1], J. Mao[2], X. Shi[2], L. Chini[3], G. Hurtt[3], and W. D. Collins[1,4]

[1]Lawrence Berkeley National Laboratory, One Cyclotron Road, MS 74R316C, Berkeley, CA, 94720.

[2]Environmental Sciences Division and Climate Change Science Institute, Oak Ridge National Laboratory, Oak Ridge, TN, USA

[3]Department of Geographical Sciences, University of Maryland, College Park, MD

[4]Department of Earth and Planetary Sciences, University of California, Berkeley, CA

Contents of this file

Additional Supporting Information (Files uploaded separately)

Introduction

The supplemental text describes two intermediate Land Use and Land Cover Change (LULCC) cases and their carbon results. Figures S1 and S2 replicate Figure 1 and half of Figure 2, including these additional cases, to demonstrate consistency across our maximum envelope range.

Figure S3 shows the spatial distribution of ecosystem carbon uncertainty and how it relates to the combination of initial carbon content and the amount of forest cover change (Figure 3a).

Figures S4 and S5 provide additional information regarding relationships between atmospheric variables and the amount of forest cover. The data for Figure S1 is also plotted in Figure 3.

The supplemental datasets contain the data plotted in Figures 1-3 and Figures S1-S5. They are model outputs that have been converted into the appropriate formats for creating meaningful figures. The processing includes averaging or aggregating monthly outputs to annual values, sometimes calculating annual averages across several years, differencing these averages, and in some cases calculating annual averages of these differences across several years.

Text S1. Two additional Land Use and Land Cover Change (LULCC) configurations represent intermediate LULCC. The commonly used "Pasture rule" preferentially converts grass and shrubs upon pasture expansion and reverts land back to potential vegetation proportionally to the available potential Plant Functional Type (PFT) coverage. A complementary "Crop rule" preferentially converts forest upon cropland expansion and reverts land back to potential vegetation proportionally to the available potential PFT coverage. The results of these two cases are expectedly within the maximum envelope (Figures S1 and S2). Constraining the uncertainty range to these intermediate cases gives a final forest area difference of 2.28 M km^2, a 30 PgC range of cumulative net LULCC emissions (57% of CO_2 plus climate), and a final difference in ecosystem carbon of 19 PgC (46% of CO_2 plus climate).

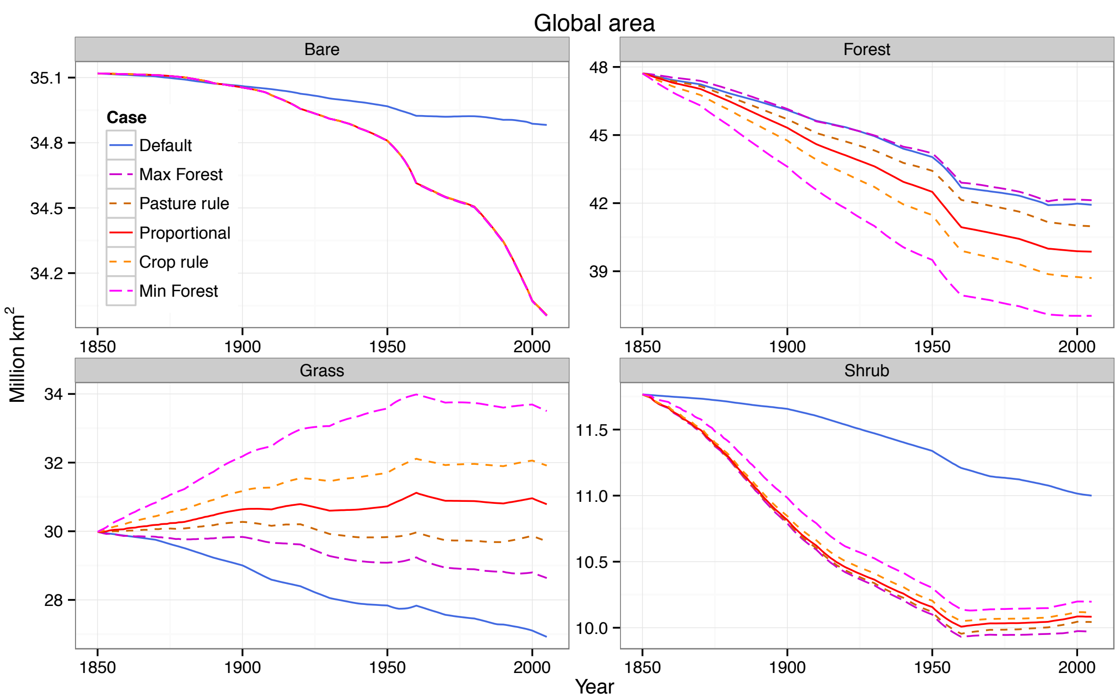

Figure S1. Global plant functional type (PFT) areas for half-degree, land-only simulations in Table 1 and the two additional cases described in Text S1. The No LULCC case maintains 1850 areas through 2005 for all PFTs. Crop area is the same for all cases except No LULCC.

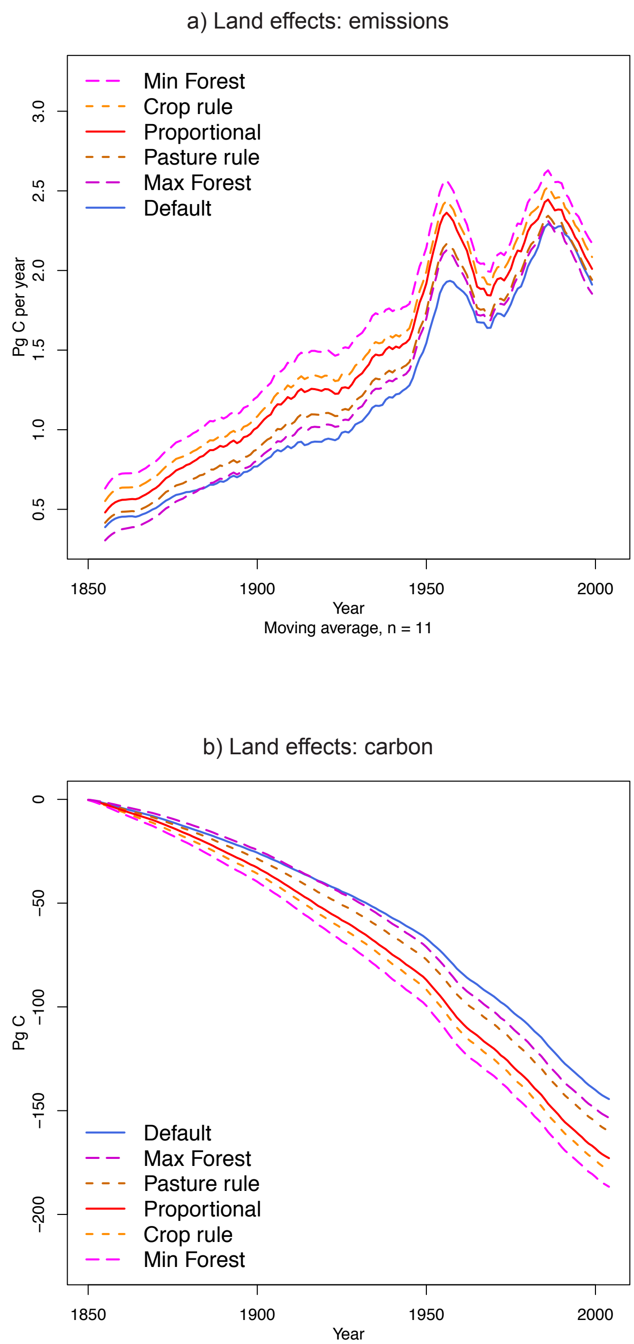

Figure S2. Effects of Land Use and Land Cover Change (LULCC) uncertainty on terrestrial carbon for the land-only simulations in Table 1 and the two additional simulations described in Text S1. Effects of a) land cover uncertainty on net annual LULCC emissions and b) land cover uncertainty on change in total ecosystem carbon due to LULCC. Emission values are 11-year running averages of the difference between each LULCC case and the No LULCC case of: net ecosystem exchange minus natural fire emissions. Ecosystem carbon values are the differences between each LULCC case and the No LULCC case.

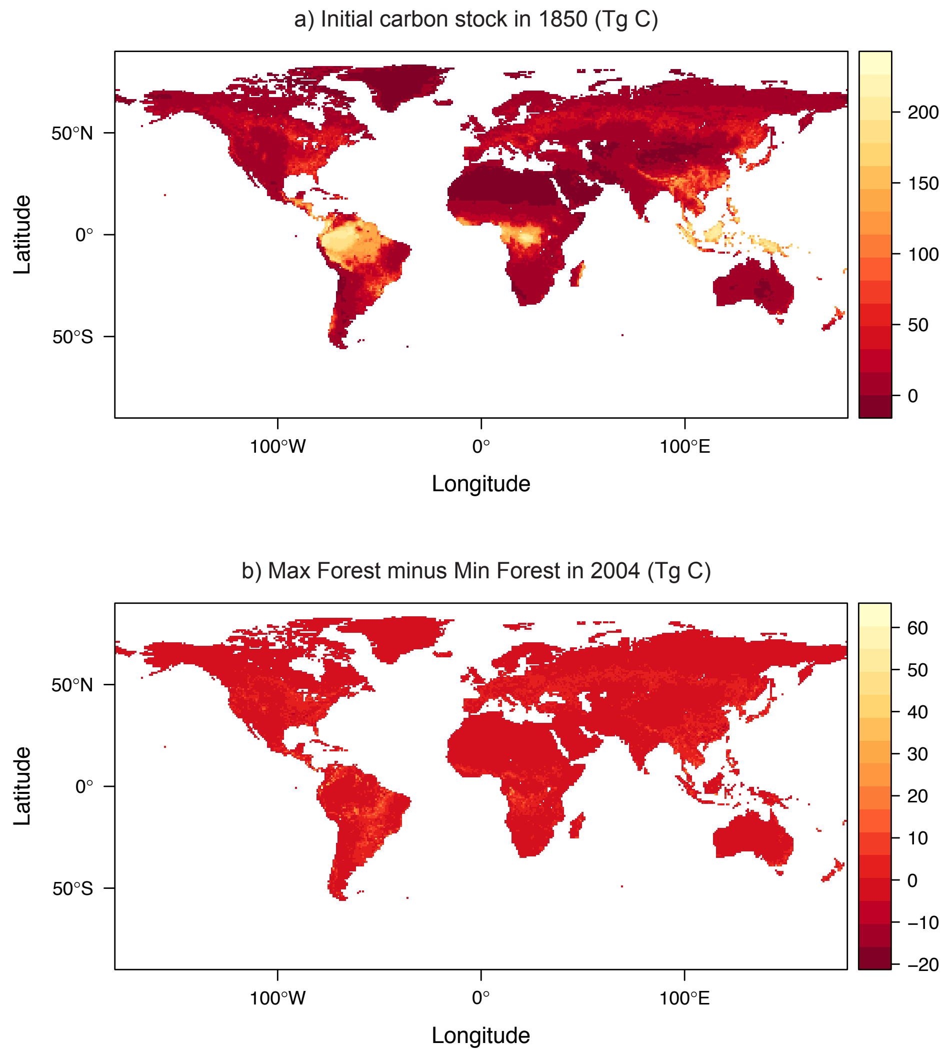

Figure S3. Spatial distributions of a) initial ecosystem carbon stocks (1850 average) and b) 2004 ecosystem carbon uncertainty range due to land cover conversion assumptions (Tg C). The spatial distribution of uncertainty is dependent on the amount of forest cover difference (Figure 3a) and the carbon content (Figure S3a).

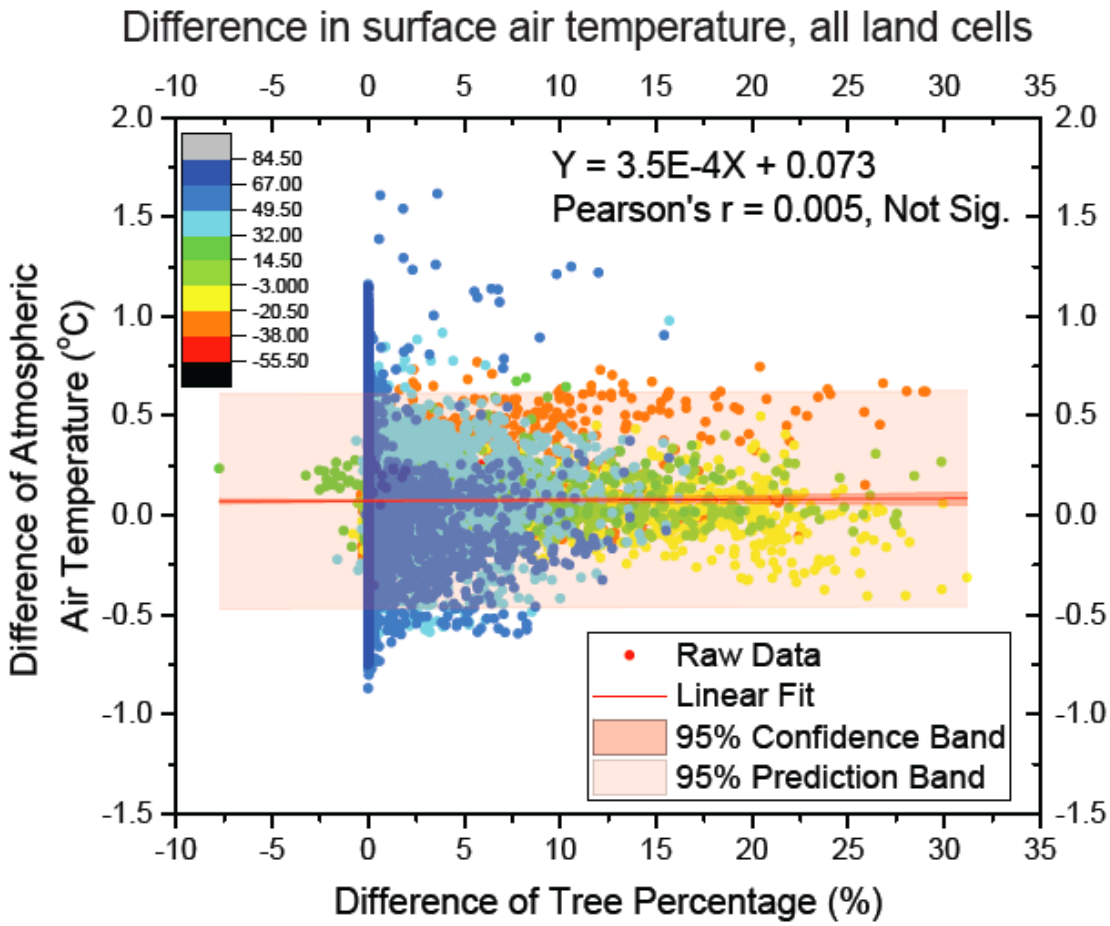

Figure S4. Sensitivity of surface air temperature to difference in tree cover (Max Forest minus Min Forest, as percent of grid cell). These values are the differences between the 20-year annual averages (1985-2004).

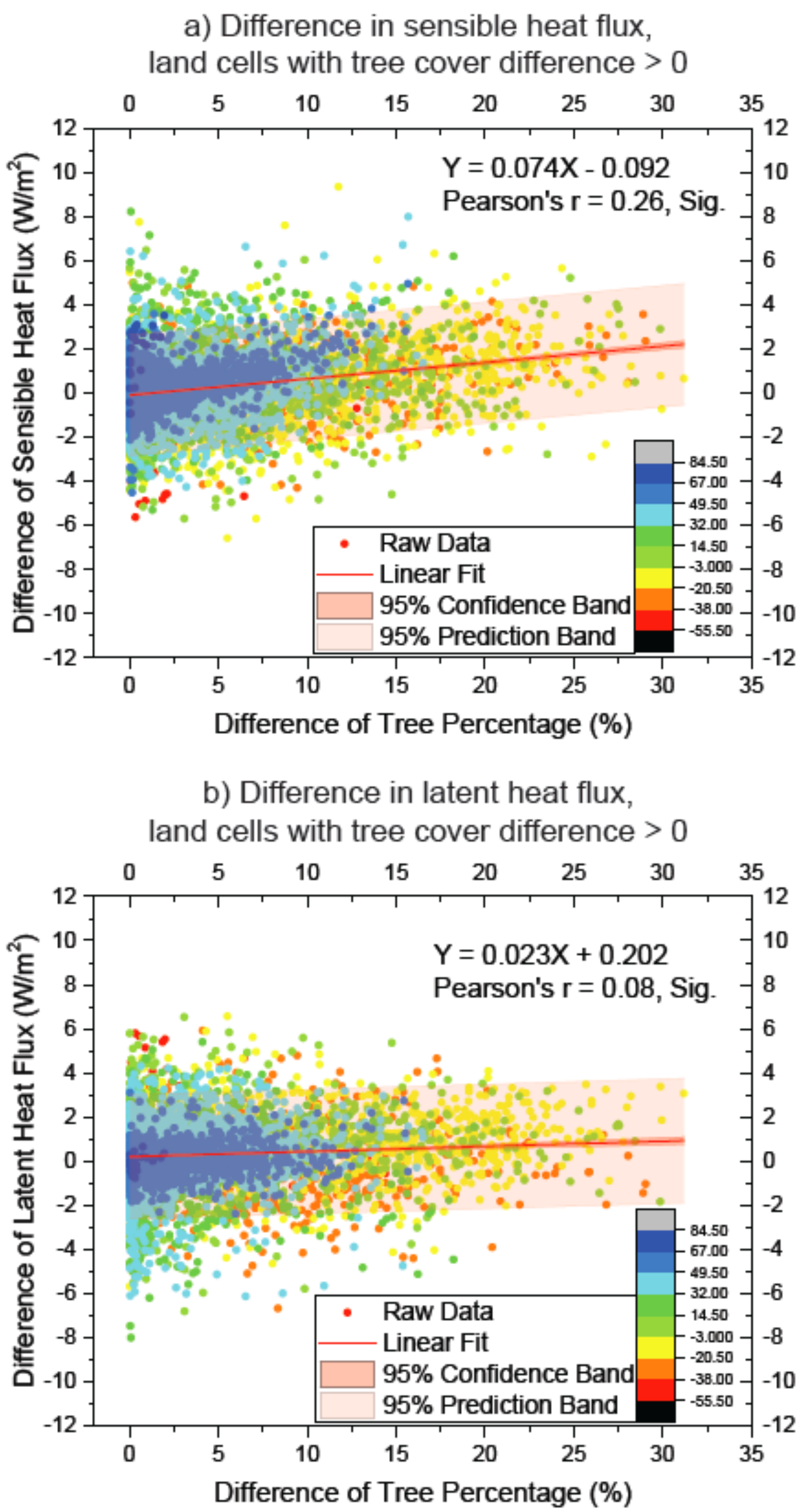

Figure S5. Sensitivity of (a) sensible heat flux, and (b) latent heat flux to difference in tree cover (Max Forest minus Min Forest, as percent of grid cell). These values are the differences between the 20-year annual averages (1985-2004).

Data Set S1. Global plant functional type area for the half-degree, land-only simulations corresponding to the land cover conversion assumptions in Table 1. These data are plotted in Figure 1.

Data Set S2. The effects of Land Use and Land Cover Change (LULCC) uncertainty and atmospheric forcing on terrestrial carbon. These data are plotted in Figure 2.

a) Net direct annual Land Use and Land Cover Change (LULCC) carbon emissions for different land cover trajectories. The values are the 11-year running average of the difference between each LULCC case and the No LULCC case of: net ecosystem exchange minus natural fire emissions. These data are plotted in Figure 2a.

b) Net direct annual Land Use and Land Cover Change (LULCC) carbon emissions for different atmospheric forcings. The values are the 11-year running average of the difference between each LULCC case and the No LULCC case of: net ecosystem exchange minus natural fire emissions. These data are plotted in Figure 2b.

c) Change in total ecosystem carbon due to Land Use and Land Cover Change (LULCC) for different land cover trajectories. The values are the difference between each LULCC case and the No LULCC case. These data are plotted in Figure 2c.

d) Change in total ecosystem carbon due to Land Use and Land Cover Change (LULCC) for different atmospheric forcings. The values are the difference between each LULCC case and the No LULCC case. These data are plotted in Figure 2d.

Data Set S3. Global plant functional type area for the half-degree, land-only simulations corresponding to the land cover conversion assumptions in Table 1, plus the two additional cases described in Text S1. These data are plotted in Figure S1.

Data Set S4. The effects of Land Use and Land Cover Change (LULCC) uncertainty on terrestrial carbon for the cases in Table 1 plus the additional cases described in Text S1. These data are plotted in Figure S2.

a) Net direct annual Land Use and Land Cover Change (LULCC) carbon emissions for different land cover trajectories. The values are the 11-year running average of the difference between each LULCC case and the No LULCC case of: net ecosystem exchange minus natural fire emissions. These data are plotted in Figure S2a.

b) Change in total ecosystem carbon due to Land Use and Land Cover Change (LULCC) for different land cover trajectories. The values are the difference between each LULCC case and the No LULCC case. These data are plotted in Figure S2b.

Data Set S5. Per-pixel a) initial carbon stocks (TgC; 1850 average) and b) 2004 uncertainty range (TgC; Max Forest – Min Forest). The first pixel is the upper left corner with the series going row-by-row (i.e., longitude increases first). The data are half-degree resolution with upper left corner edge at -180 degrees E and 90 degrees N, and with 360 rows and 720 columns. These data are plotted in Figure S3.

Data Set S6. Sensitivity of surface air temperature to difference in tree cover (Max Forest minus Min Forest, as percent of grid cell). These values are the differences between the 20-year annual averages (1985-2004). These data are plotted in Figures 3 and S4.

Data Set S7. Sensitivity of (a) sensible heat flux, and (b) latent heat flux to difference in tree cover (Max Forest minus Min Forest, as percent of grid cell). These values are the differences between the 20-year annual averages (1985-2004). These data are plotted in Figure S5.